Comparison of Failure Stress Distributions in Automotive Windscreens by Experiment and Simulation

Christopher Brokmann[1], Stefan Kolling[1]

[1]Institute of Mechanics and Materials, Technische Hochschule Mittelhessen, Gießen

1 Abstract

Due to the stochastic fracture behaviour of glass, a large scattering is to be expected when determining injury criteria (e.g. HIC) in the case of a pedestrian head impact on an automotive windscreen. In addition, the origin of failure is difficult to determine as the strength of glass depends on initial flaws within the material and their growth rate. Since these flaws are randomly distributed over the entire windscreen, a prediction of the crack origin is only possible to a limited extent. Further factors that may have a statistical significance, for example the point of impact or the shape and material parameters of the windscreen, have hardly been investigated so far.

This investigation presents a methodology to determine experimentally the fracture stress from windscreens. Subsequently, they are compared to values from finite element (FE) simulations using LS-DYNA. For this purpose, the laminated glass is subjected to quasi-static loading in a head impact replacement test where a pedestrian adult head is pushed to the windscreen. The origin of the initial fracture was found by acoustic emission (AE) localisation. The evaluated origins of failure were examined for fracture marks, particularly for the fracture mirrors. These have a direct relation to fracture stresses by a material constant, which can be used to determine experimentally fracture stresses of brittle materials.

FE Simulations of the pedestrian head impact replacement test on the windscreen were carried out. With the data from the acoustic emission localisation, stresses at the calculated fracture origins were evaluated from the simulations. For both, the numerical and experimental fracture stresses, statistical investigations were performed. It could be shown that the determined stresses from experiments and simulations are well comparable and thus represent a reliable basis for future stochastic simulations.

A comprehensive version of this extended abstract can be found in [1].

2 Experimental Investigation

2.1 Head Impact Replacement Test

In the present work, we set our focus on estimation of the fracture strength of windscreens under low velocity impact. The capability of small-scale tests of single glass ply, for example four-point bending or coaxial double ring tests, are limited by possible influences of windscreen manufacturing, e.g. bending, edge grinding and handling. The edge and surface strength are also difficult to determine on small samples out of windscreens due to the curvature of the windscreens [2]. An alternative approach to determine the strength for non-linear geometries is the method presented in this investigation using AE localisation and fracture mirror analysis. For this purpose, a quasi-static head impact replacement test is utilised, where the impactor is pushed displacement-controlled to the windscreen by an electrical cylinder. As head impactor, shown in Fig. 1, we use the adult head form according to the Euro NCAP pedestrian testing protocol [3] where the spherical impactor is 136 mm in diameter including a 14 mm thick rubber skin which simulates the behaviour of the human skin. The tested laminated glass structures consist of Mercedes C-Class windscreens in immaculate condition, directly from the manufacturer. The windscreens are made of two 1.8 mm thick soda-lime silica float glass ply, bonded with a 0.76 mm PVB interlayer. The head impactor hits the windscreens 340 mm below the top edge, in the horizontal middle of the windscreen. Fig. 2 shows one of the tested windscreens with the coordinate system used for AE localisation. The black areas on the windscreen were dyed using a silkscreen process. The test setup is made of a massive steel frame with four point supports for the windscreens, shown in Fig. 1. Each support consists of a half-sphere made of PVC with a diameter of 36 mm. The purpose of the selected four-point support is to measure purely the glass properties and to eliminate possible influences of the adhesive in glued-in conditions. To reduce further influences, the windscreens do not have any
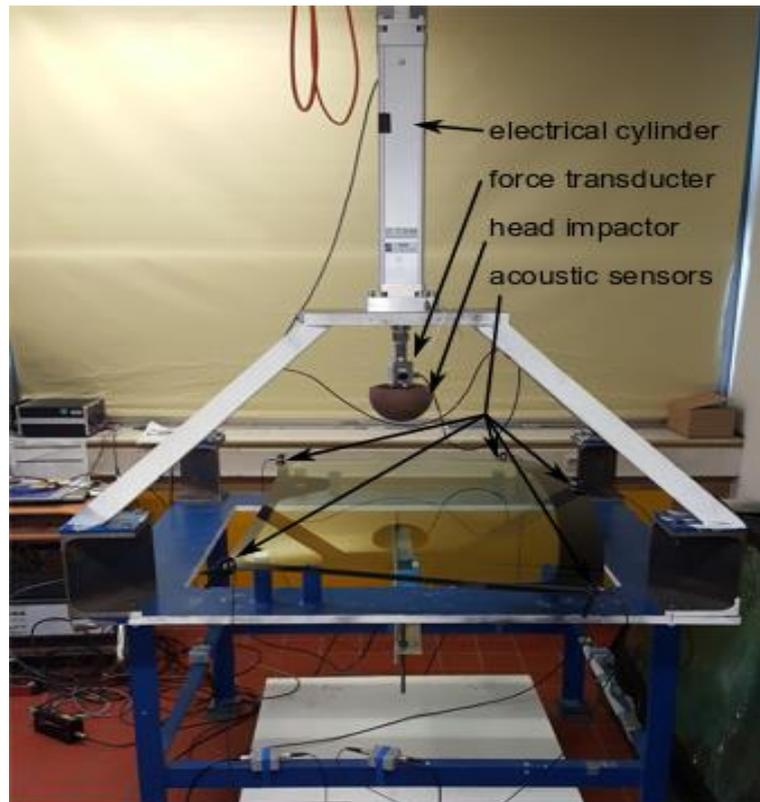
Fig.1: Experimental test setup

additional components such as rear-view mirrors or heating wire. Especially when comparing the fractographic strengths with the corresponding values from FE analysis, the influence of the visco-hyperelastic material behaviour by the adhesive would be difficult to characterise. The intent of this study is to investigate the behaviour of glass and not the behaviour of a complete component. Furthermore, the material behaviour of the adhesive is difficult to keep constant during experiments done over a long-time period. Future investigations will have to show if these strengths can be compared with those from a boundary with continuous support on adhesive bed. With respect to the fracture pattern, the four-point boundary is not usable. However, the content of this manuscript is the determination of failure stresses not the fracture pattern. The electrical cylinder, type EMC 100-40 from Bosch Rexroth AG, is also fixed with the steel frame. The impact replacement tests are carried out at a constant loading speed of 0.01 m/s. The entire experimental setup was designed and validated in [4].
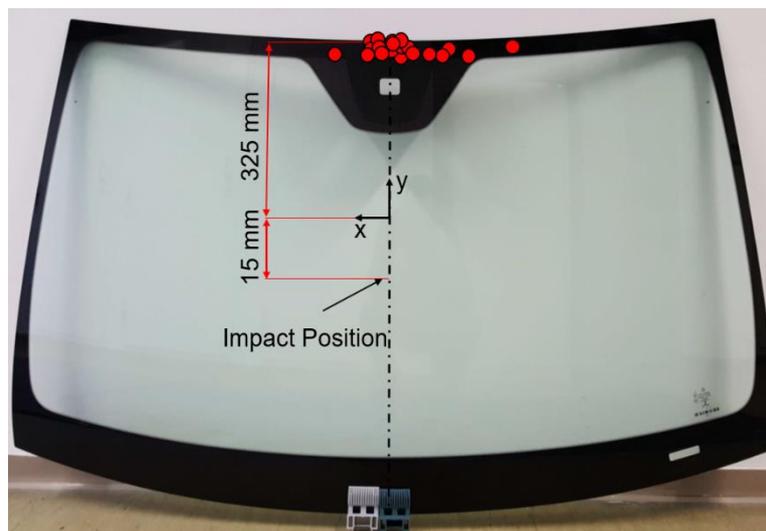

Fig.2: Tested windscreen with coordinate system and point of impact

2.2 Acoustic Emission Localisation

Due to a random fracture pattern of laminated safety glass windscreens after failure, the origin of failure is complex to find by optical examination. An exact localisation is also of great importance for the comparison with a FE simulation, since the measured stress value can be subjected to a certain error due to a high stress gradient.

For this purpose, AE analysis were performed with a total of five AE sensors. The AE measures acoustic waves passing through the observed medium. In the present case, this occurs in the event of sudden relief of strain energy through failure. There are several possible algorithms to determine the signal source [5][6]. Within the following experiments, the time difference of arrival method (TDOA) is used. The TDOA measures the incoming signal by the arrival time at the sensors and is especially useful for events of unknown initial event time.

By the time difference $\Delta t_{ij} = |t_i - t_j|$ of the incoming signal between two AE sensors i and j, multiplied with the speed of sound v_s of the observed material, a difference in distance Dd can be calculated. For a sensor pair i and j, the signal source must be at the measured distance difference. This can mathematically be expressed by a hyperbolic function as

$$\Delta d_{ij} = \sqrt{y^2 + \left(x + \frac{x_i}{2}\right)^2} - \sqrt{y^2 + \left(x + \frac{x_j}{2}\right)^2},$$

assuming that the location of the AE sensors s_i and s_j are at $s_i(x_i|0)$ and $s_j(x_j|0)$ with $x_i = x_j$ or $\Delta x = 2x$. With some simplifications, Δd_{ij} can be expressed by

$$\frac{x^2}{\left(\frac{\Delta d}{2}\right)^2} - \frac{y^2}{\left(\frac{\Delta x}{2}\right)^2 - \left(\frac{\Delta d}{2}\right)^2} = 1,$$

which is similar to the canonical form of a hyperbola. In order to compare the hyperbola of one AE sensor pair with other ones, the coordinates of the hyperbola (x,y) need to be translated into a global coordinate system (X,Y) by

$$\begin{pmatrix} X \\ Y \end{pmatrix} = \begin{pmatrix} \Delta X \\ \Delta Y \end{pmatrix} + \begin{pmatrix} \cos(\alpha) & \sin(\alpha) \\ -\sin(\alpha) & \cos(\alpha) \end{pmatrix} \begin{pmatrix} x \\ y \end{pmatrix}$$

with α as the angle and ΔX, ΔY as the offsets between both coordinate systems. The total number of hyperbolas n_{hyp} increases with the number of sensors n by

$$n_{hyp} = \sum_{i=1}^{n} (i - 1)$$

Fig. 3 shows the TDOA procedure graphically with two sensors and one corresponding hyperbola. Note that interference factors and measurement uncertainties do not lead to an exact intersection of all hyperbolas. To solve this issue, the calculated hyperbolic functions are iterated by adjusting the measured arrival times and minimizing a **l**ocation **unc**ertaint**y** value (LUCY), which is calculated by
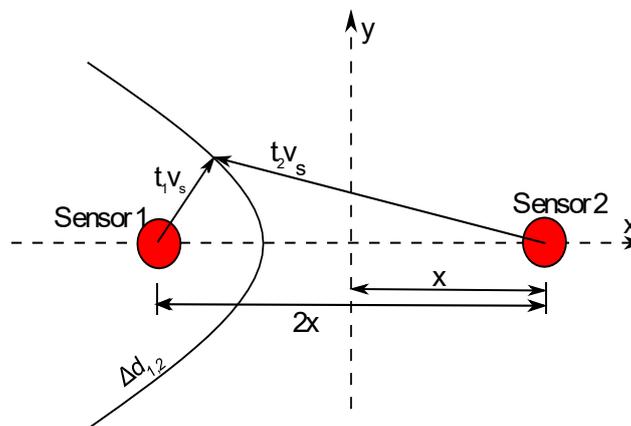

Fig.3: TDOA procedure with two sensors

$$LUCY = \sqrt{\frac{\sum_n \left(\Delta d_{ij} - \Delta p_{ij}\right)^2}{n-1}}$$

where Δd is the first calculated and Δp the adjusted distance between the sensors. The calculated values are obtained by a gradient algorithm in which the measured arrival times are adjusted. A high LUCY value indicates accordingly a high difference between the measured and calculated values. The LUCY value in the performed experiments was always lower than ten millimetres. The validity of LUCY as a location uncertainty criterion has already been investigated [7]. For the application of acoustic emission analysis on automotive windscreens, this criterion and its quality should be subject of future investigations. Fig. 4 shows an example of AE localisation via TDOA method. The results from AE localisation during experiments are shown in Tab. 1.
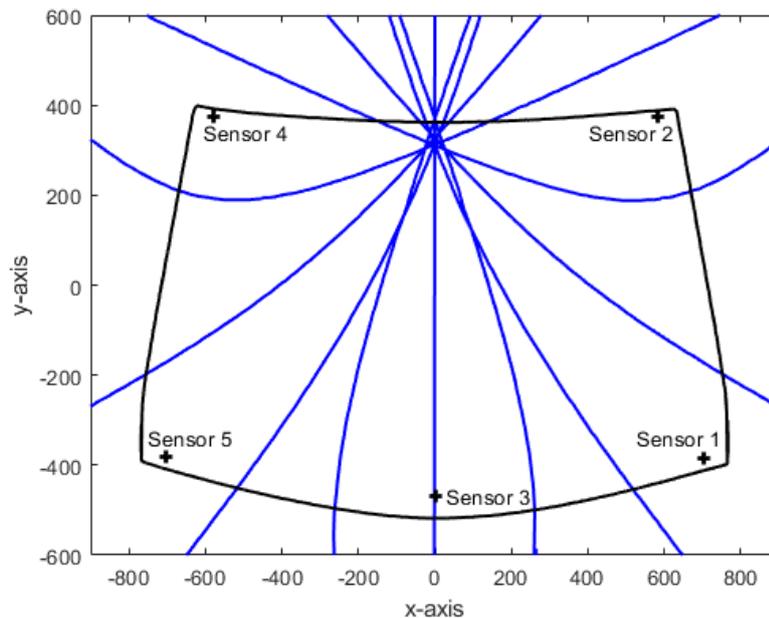

Fig.4:   TDOA localisation from a Mercedes C-Class Windscreen

2.3   Fractographic Stress Evaluation

At the localized points of initial failure, the crack flanks were scanned for the so-called fracture mirror in order to be able to calculate the failure stresses σ_f with

$$\sigma_f = Ar^{-0.5}$$

where r is the mirror radius and A is the so-called "mirror constant" which can be assumed as a material constant [8][9]. Fig. 5 shows two fracture mirrors with the radii r. The mirror constant for soda-lime silica float glass, which was chosen for the examined windscreens, is A=1:8 MPa√m [10]. It is advisable to determine the fracture mirror constant for the given material oneself, since literature values are subject to a certain variation, see e.g. [9]. The stresses could be estimated between 58.48 MPa and 100.51 MPa with A = 1:8 MPa√m as constant value. These values are listed in Tab. 1. The mirror radii are always from the bottom glass ply in the screen-printed area at side four, the interior side. The bottom ply is chosen for investigations due to the fact, that this ply mostly breaks first. The evaluation of fracture mirrors is generally assumed to have an inaccuracy for the radii through experience of the fractographer, the microscopy and selected illumination. The determination of stresses by fracture mirrors is assumed to be up to ten percent inaccurate for symmetrical shaped fracture mirrors [9].
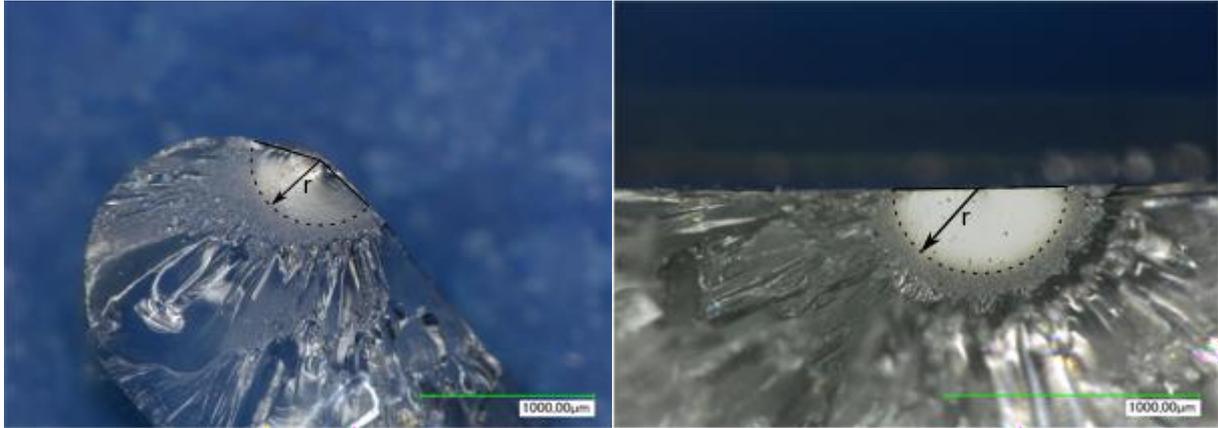
Fig.5:   Two fracture mirrors from Mercedes C-Class windscreens after failure

3 Numerical Investigation

A FE calculation is performed to show the stress variation during the head impact experiments. The chosen FE modelling technique is a coincident shell-solid-shell coupling method [11] with an average element length of 10 mm. This coupling method merges the geometric shell nodes to the solid nodes on the upper and lower surface. To maintain the physical geometry of the windscreen, the mid surface gets shifted to the outer side by half of the element thickness (**NLOC**=1/-1), as shown in Fig. 6 and Fig. 7. The material behaviour of the PVB interlayer is described by the Blatz-Ko rubber model ***MAT_007** for the present test velocity and room temperature [12]. Both glass plies were defined as linear elastic ***MAT_001**.
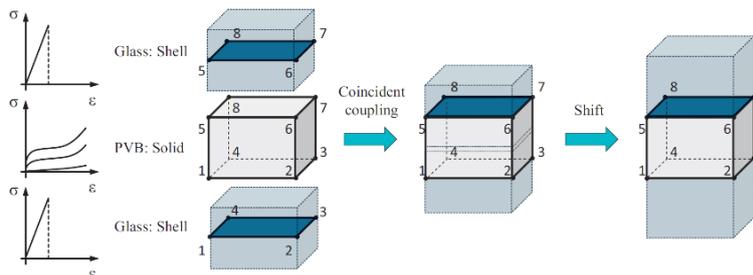

Fig.6:   Coincident coupling of laminated safety glass

The shell elements for the glass plies are modelled as fully integrated, four node shell elements (**ELFORM**=16) with five integration points through the shell thickness. The Gauss-Lobatto integration algorithm is used, with the advantage of integration points directly on the surface of the shell elements. Therefore, no stress extrapolation to the element surface is necessary, on which the experimental stresses were measured. The PVB interlayer consists of selective reduced solid elements with eight integration points (**ELFORM**=2). A FE model of the impactor, shown in Fig. 8, is used that has been validated for impact simulations in [13] and [14] respectively using the tabulated Ogden approach in ***MAT_181**, see [15]. The simulation is performed with a Young's modulus of 70 GPa for glass and a constant shear modulus for PVB of 1.4 MPa. The four-point support is modelled as rigid ***MAT_RIGID**.
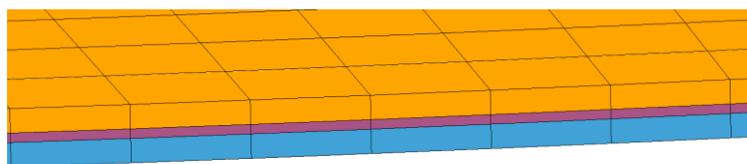

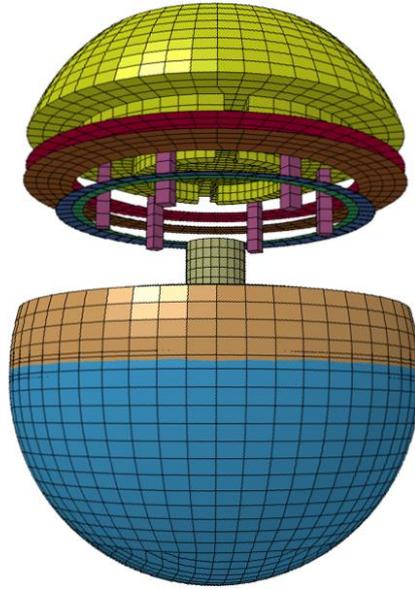*Fig.7:   Shell-solid-shell windscreen model*

Fig.8:   FE model of the head impactor

Fig. 9 shows the measured force-displacement curves from experiments in comparison to the simulation. Since the experiments were carried out using a displacement prescribed by the cylinder, the simulation was also set up with a prescribed displacement for the impactor. Accordingly, the measured displacement and impactor displacement are equal experiments and simulation. The occurring forces were measured by a force transducer between head impactor and cylinder in experiments. In the simulation, the contact forces between the windscreen and impactor were used. The curves are cut off at windscreen failure, as only the pre-failure behaviour is of importance in this investigation.

The numerical failure stresses are determined by comparing the displacement at failure from experiments with the numerical stress at this state. Since the acoustic emission localisation used for determination of the fracture origin in experiments is subjected to an uncertainty, we measured the maximum principal stresses in all elements within the uncertainty radius and calculated a mean value. The maximum and minimum principal stresses in all considered elements are also listed in Tab. 1.
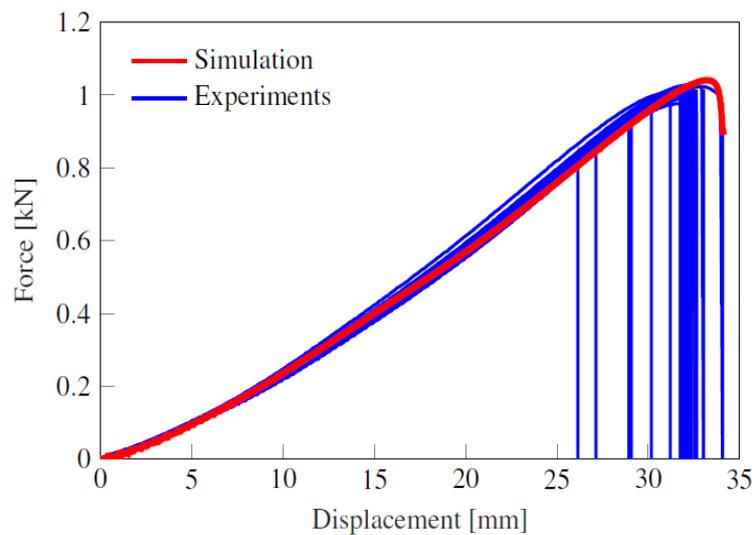

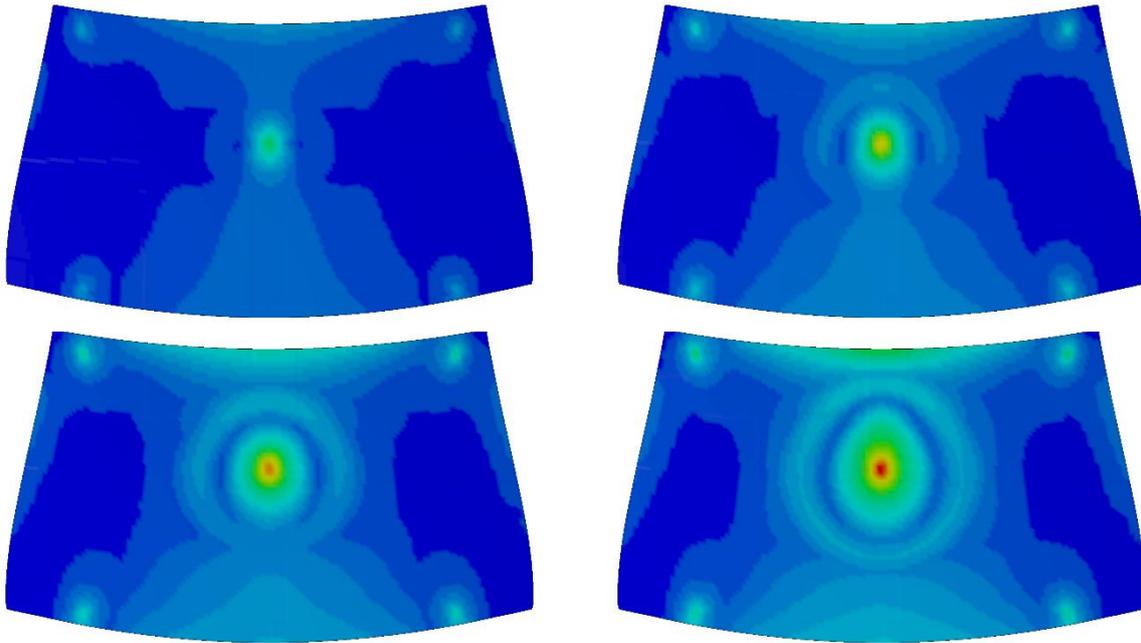*Fig.9:   Force versus displacement curves*

Fig.10: Maximum principle stress evolution, view from the interior side

The stresses are between 58.48 MPa and 100.51 MPa for experimental and 55.40 MPa to 111.05 MPa for numerical values. The highest deviation can be seen at test number 15 with 16.98 MPa. The arithmetic mean deviation between experimental and numerical stresses in all 20 experiments is 6.2 MPa. This value shows a good agreement with regard to the inaccuracy of measuring fracture mirrors [16] and numerical deviations. Fig. 10 shows the evolution of the maximum principle stress at the interior side, as defined as glass ply two, windscreen side four. While the highest stress is directly underneath the impactor, failure occurred solely at the top edge. This illustrates the reduced strength of the glass ply at the edge and in the screen-printed area.

Table 1: Location results and stresses from experiments and simulation (coordinate system in Fig. 2)

Nr.	X [mm]	Y [mm]	LUCY [mm]	σ_{exp} [MPa]	σ_{sim} [MPa]	$\Delta\sigma$ [MPa]	$\sigma_{sim,max}$ [MPa]	$\sigma_{sim,min}$ [MPa]
1	-0.78	323.04	8.29	84.89	85.10	-0.21	90.52	79.68
2	0.96	322.34	8.55	59.78	58.55	1.23	61.70	55.38
3	-36.35	318.62	7.70	99.16	111.05	-11.89	123.03	99.71
4	-1.71	322.81	8.56	81.50	80.22	1.28	85.15	75.33
5	-1.25	316.76	7.00	83.39	83.28	0.11	88.51	78.06
6	0.15	321.07	8.18	76.30	75.76	0.54	80.25	71.25
7	-1.83	320.83	8.14	73.97	65.66	8.31	69.33	61.97
8	-0.08	320.83	9.01	93.29	85.86	7.43	91.36	80.36
9	-2.64	320.37	7.50	58.48	55.40	3.08	58.35	52.44
10	-21.59	317.93	7.60	82.69	81.78	0.91	87.40	76.16
11	0.78	321.88	5.79	72.78	70.43	2.35	74.44	66.40
12	-0.66	320.25	8.57	97.59	81.19	16.40	86.18	76.20
13	3.34	316.53	7.53	100.27	85.87	14.40	91.48	80.27
14	-4.73	318.51	7.87	92.78	79.00	13.78	83.86	74.14
15	-55.76	322.81	8.33	100.51	83.53	16.98	85.31	47.48
16	-27.86	321.07	7.40	98.44	84.21	14.23	89.96	77.76
17	-0.08	320.48	8.45	99.06	90.48	8.58	96.53	84.41
18	23.10	314.90	8.54	95.47	85.13	10.34	90.60	79.16
19	-2.29	325.95	8.20	67.13	65.08	2.05	68.71	61.46
20	-0.03	321.30	8.68	96.66	85.96	10.70	91.48	80.45

4 Statistical Treatment

To evaluate the measured failure stresses, several statistical distributions are investigated on their ability to reproduce the empirical data. Only a briefly introduction is shown here. For a more detailed statistical description we refer to the comprehensive version [1]

The two parameter Weibull distribution is widely used in failure data analysis. It consists of two parameters, the shape parameter b and the scale parameter h. The shape parameter is also known as Weibull modulus. The two parameter Weibull CDF is defined by

$$P(x) = 1 - \exp\left[-\left(\frac{x}{\eta}\right)^{\beta}\right].$$

The scale parameter η is a value for the centrality of the estimated distribution. From a visual point of view 63.21 % or 1-exp(-1) of the measured values are below the value of the scale parameter. The other Weibull parameter, the shape parameter β, is an indicator for the occurrence variance. A low shape parameter means that the measured values have a higher scatter around the mean value than it would be the case with a higher value. For the given data, the parameters can be determined as $\eta_{exp} = 91.6349$ and $\beta_{exp} = 7.0088$ for experiments and as $\eta_{sim} = 84.8881$ and $\beta_{sim} = 7.5014$ for the simulation. The parameters were obtained by linear regression.

When comparing the parameters of simulation and experiment, it is noticeable that the scale parameter from the simulation is about 6.75 MPa lower than the experimental one. The simulation values also have a higher shape parameter and thus a lower scatter.

Fig. 11 shows the measured failure stress values within the two parameter Weibull plot. For a better representation, the linearized form of the two parameter Weibull distribution is shown, where ln [- ln(1 - P(x))] is drawn on the ordinate and ln(x) to the abscissa. The parameter of the linear function y = a x+b can then be expressed by the Weibull parameters to a = β and b = -ln(η) a.

For a linear regression, approaches exist to characterize the confidence for the fitted regression line and to predict another single value on a given certainty. This is shown by the confidence and prediction bounds, determined with a statistical significance of α = 0.05, which is equal to a certainty of 95 %. The upper and lower bounds for the confidence are given by

$$E[Y|x_i] = (ax + b) \pm t_{1-\alpha,n-2}s_r \sqrt{\frac{1}{n} + \frac{(x_i - \bar{x})^2}{\sum_{j=1}^{n}(x_j - \bar{x})^2}},$$

and for the upper and lower prediction bound by

$$E[Y = y_i|x_i] = (ax + b) \pm t_{1-\alpha,n-2}s_r \sqrt{1 + \frac{1}{n} + \frac{(x_i - \bar{x})^2}{\sum_{j=1}^{n}(x_j - \bar{x})^2}},$$

The value t expresses the tabulated Student's t-distribution value for the used significance α = 0.05 and n - 2 degrees of freedom. The variance for the regression was determined by
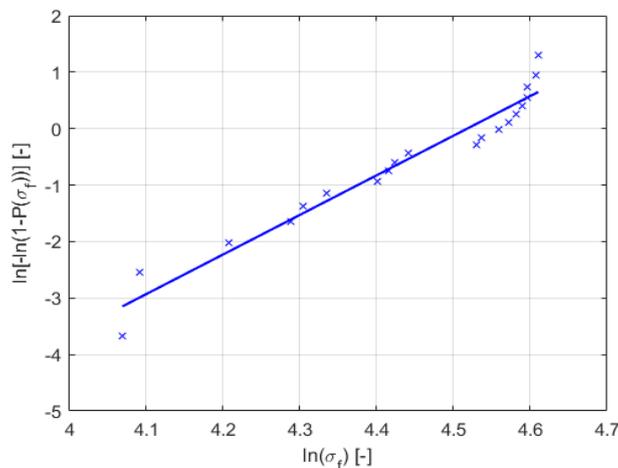

Fig.11: Experimental stresses within a two parameter
Weibull distribution

$$s_R = \sqrt{\frac{\sum_{i=1}^{n}[y_i - (ax_i + b)]^2}{n - 2}}$$

The prediction bounds are an estimate of the interval in which future failure stresses will occur. The confidence interval means, that there is a 95 % probability that the real linear regression lies within the confidence limits for the given data.

5 Conclusion

In the present investigation, an experimental methodology has been suggested as a combination of acoustic emission localisation and fractography to determine failure stresses out of laminated safety glass. With the present method, it is possible to obtain experimentally the failure stresses from brittle components with non-linear geometries.

This method was used to determine the probability distribution of failure stresses during a quasi-static head impact on automotive windscreens. It could be shown, that the measured stresses can be assumed to be two parameter Weibull distributed.

By using the experimental data and a finite element analysis, numerical failure stresses could be calculated. Additionally, we could show, that the Weibull parameters from experiment and simulation are in good agreement.

The localized failure origins were always in the coated area near or at the edge. While the influence from production processes on the edge strength and the flaw density is well known, the influence from the production process of the screen printing for glass is still not completely analyzed and therefore becomes the topic of further investigations.

6 Literature

[1] Brokmann, C., Alter, C. and Kolling, S.: „Experimental determination of failure strength in automotive windscreens using acoustic emission and fractography". Glass Struct Eng, 2018, 1-13.

[2] Müller-Braun, S. and Schneider, J. "Biaxially curved glass with large radii-determination of strength using the coaxial double ring test". Glass Struct Eng, 2, 2017, 121–131.

[3] Euro NCAP. Pedestrian testing protocol, 2018.

[4] Kolling, S., Alter C., and Rühl. A. "Experimentelle und Numerische Untersuchungen von Windschutzscheiben unter stoßartiger Belastung zur Verbesserung des Fußgänger-und Insassenschutzes." Abschlussbericht BMBF Projekt 17N1111, 2015.

[5] Liu, Y., et al. "Location, localization, and localizability." Journal of Computer Science and Technology 25.2, 2010, 274-297.

[6] Grosse, C. U., and Ohtsu, „Acoustic emission testing". Springer Science & Business Media, 2008.

[7] Thenikl, T., Altmann, D. and Vallen H.. "Quantifying Location Errors." 32nd European Conference on Acoustic Emission Testing, 2016.

[8] Fréchette, V. D.. "Failure analysis of brittle materials.", 1990.

[9] Quinn, G. D., and Quinn, G.D. "Fractography of ceramics and glasses." National Institute of Standards and Technology Washington, DC, 2007.

[10] Ball, M. J., Landini D. J., and Bradt R. C. "Fracture mist region in a soda-lime-silica float glass." Fractography of Ceramic and Metal Failures. ASTM International, 1984.

[11] Alter, C., et al. "Lokalisierung des initialen Versagens bei Verbundsicherheitsglas unter stoßartiger Belastung." Stahlbau 84.S1, 2015, 433-442.

[12] Du Bois, P. A., Kolling S., and Fassnacht W. "Modelling of safety glass for crash simulation." Computational materials science 28.3-4, 2003, 675-683.

[13] Frank, T., et al. "Development and validation of numerical pedestrian impactor models." 4th European LS-DYNA Users Conference. 2003.

[14] Du Bois, P. A., et al. "Material behaviour of polymers under impact loading." International Journal of Impact Engineering 32.5, 2006, 725-740.

[15] Kolling, S., et al. "A tabulated formulation of hyperelasticity with rate effects and damage." Computational Mechanics 40.5, 2007, 885-899.

[16] Ma, Lingyue, Roberto Dugnani, and Ricardo Zednik. "Quantifying the Accuracy of Fractographic Strength Estimates in Silicate Glasses." Journal of the European Ceramic Society 38.10, 2018, 3643-3649.